Journal of Magnetic Resonance **144,** 85–88 (2000)
doi:10.1006/jmre.2000.2014, available online at http://www.idealibrary.com on IDEAL®

# An L-Band Crossed-Loop (Bimodal) EPR Resonator

George A. Rinard, Richard W. Quine, and Gareth R. Eaton

*Department of Engineering and Department of Chemistry and Biochemistry, University of Denver, Denver, Colorado 80208*

Received September 1, 1999; revised December 27, 1999

**Our crossed-loop resonator design has been enhanced to increase the filling factor and has been extended from S-band to L-band. High isolation between the two modes results in shorter dead time in pulsed EPR experiments than would occur with a reflection resonator of the same *Q*.** 

## INTRODUCTION

High isolation between the microwave source power and the EPR signal enhances the ability to measure dispersion CW EPR and to measure short-time responses in pulsed EPR. To achieve high isolation, several groups have produced bimodal resonators (*1–19*). The background literature has been reviewed comprehensively (*7, 10, 11, 16, 20, 21*). Most of these resonators were developed for a special, restricted application and would not serve as models for a general-purpose biomedical EPR resonator. The best-known of these is Hyde's dual rectangular resonator (with crossed $TE_{102}$ and $TE_{103}$ modes in various combinations) (*4–7, 10*). A detailed description of the Varian Associates bimodal E-802 ELDOR cavity (*8*) was published by Leniart (*11*).

The Mailer *et al.* $TM_{110}$ bimodal cavity was designed specifically for aqueous biological samples in 1-mm-diameter capillary tubes and had isolation of ca. 37 dB between modes, which reduced the effect of source noise in low-power CW experiments for nitroxyl radicals (*12*). Barendswaard *et al.* used a bimodal cavity based on the patented Biehl and Schmalbein resonator (*14*) design to reduce dead time in ESE experiments to as small as 30 ns at X-band (*13*). This resonator has two coaxial somewhat overlapping cylindrical resonators. The sample had to be located exactly at the intersection of the horizontal and vertical mirror planes of the cavity. If the sample was nonconducting, the decoupling of the two modes could be made as high as 80 dB by using sliding metal brushes as "tuning paddles." Without such adjustments, the isolation was about 35 dB, and even with adjustment the isolation was 65 dB when the sample was conducting (*13*). Other dual-mode resonators have been used for microwave Hall effect measurements, using instruments very similar to EPR spectrometers (*22*).

The development of lumped-element resonators, such as the loop–gap resonators (LGR), provides a new basis for designing bimodal resonators. A concept for a bimodal LGR was proposed (*15*) and constructed in a test-bench version that has an active volume of 2.7 $mm^3$ (*16*). Test-bench data showed isolation of 35 dB between the two modes. It was predicted that bimodal resonators based on the LGR geometry would be easier to use and less microphonic than bimodal cavity resonators (*15*). Hyde's 1995 bimodal LGR has parallel or antiparallel, rather than orthogonal, fields and achieves isolation between modes by tuning such that the integral over space of the scalar product of the two modes is zero (*15, 17*).

In 1996 we described an S-band bimodal resonator that we call a crossed-loop resonator (CLR) to emphasize that the resonator consists of two loop–gap resonators arranged so that the common volume, where the sample is placed, is where the two resonators cross orthogonally (*18*). We showed the value of this resonator for dispersion and superheterodyne operation (*19*). We are currently extending this technology to higher and lower microwave frequencies. Except for the Piasecki, Froncisz, and Hyde S-band bimodal resonator (*17*) and our S-band CLR (*18, 19*), all bimodal EPR resonators have been made for use at X-band. In this paper we describe an L-band CLR and show that with it one can achieve dead times in pulsed EPR even shorter than are common with a reflection resonator at X-band. The performance of this CLR is enhanced by a larger reentrant loop, which increases the filling factor.

## DESIGN OF THE L-BAND CLR

The original S-Band CLR (*18*) had sample and reentrant loops that were 6 mm in diameter. The common sample volume was thus roughly spherical and 6 mm in diameter. The second-generation S-band CLR and the present L-band CLR were redesigned to enhance the sample volume and increase the filling factor. This was accomplished by increasing the size of the reentrant loops and by making one of the loops oval as shown in Fig. 1. The diameter of the sample loop in both the S- and the L-band CLRs is 4.2 mm to accommodate standard 4-mm sample tubes. The gap length (GL) and other critical dimensions are given in Table 1.

Other than the modifications described above, the construction of the CLRs is essentially the same as that described in Ref. (*18*). Both the S-band and the L-band CLRs are con-



1090-7807/00 $35.00

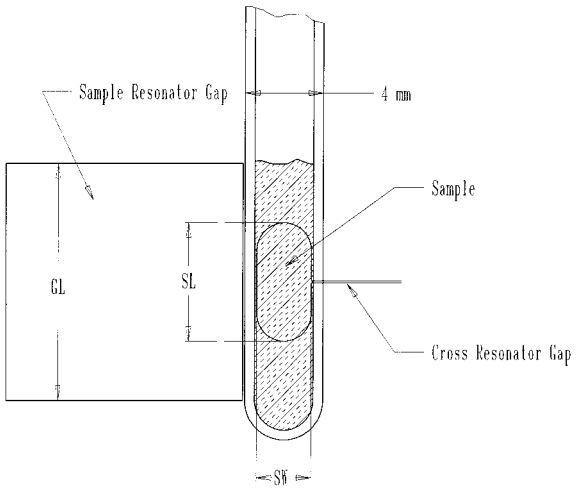


**FIG. 1.** Sketch showing the critical dimensions of the sample region of the L-band CLR; the other features of the CLR are as shown in Refs. (*18, 19*). GL is the length of the gap in the circular or sample resonator. SL and SW are the effective sample length and width that are seen by the orthogonal oval loop resonator. Only the sample in this region produces an EPR signal.

structed of Te–Cu alloy 145 and are gold plated. The gold plating reduces the *Q* of the resonator somewhat. The reentrant loop on the L-band CLR has a cross-sectional area about seven times that of the sample section. Since the integral of $B_1^2$ is inversely proportional to the cross-sectional area, the larger reentrant loop improves the filling factor. The reentrant loop of the S-band CLR is somewhat smaller because of constraints to fit into a particular cryostat, but the ratio of SL to GL (Fig. 1) is somewhat larger. The filling factors for the sample loops of the L- and S-band CLRs are estimated to be 11 and 12%, respectively. The two sections of the CLR are constructed so that they can be rotated relative to one another so that their magnetic fields can be maintained orthogonal even with sample changes.

The resonant section with the round loop (sample loop) has a fixed resonant frequency. The section with the oval loop has a frequency tuning screw that effectively changes the capacitance of the gap for this resonator and allows the frequency to be tuned over about a 5% range. This allows both sections to be tuned to the same frequency while compensating for the effects of overcoupling and loading due to the sample and sample tube.

## PERFORMANCE TESTS

At critical coupling, the fixed-frequency section, when empty, resonated at 1.926 GHz. The empty variable-frequency resonator had a maximum frequency of 1.911 GHz. With a sample tube in the CLR, the resonant frequency of the fixed-frequency section decreases more than that of the variable-frequency section, and both loops can be tuned to the same frequency at critical coupling. This allows the maximum offset frequency of the variable-frequency section for applications requiring different resonant frequencies.

A crucial performance check of the L-band CLR was to compare its performance with an S-band CLR. The dimensions of this S-band CLR, which is smaller than the one reported in (*18, 19*) so that it could fit into a cryostat, are given in Table 1 for comparison. A two-pulse echo measurement was made using a standard irradiated fused $SiO_2$ sample (*24*) and 60, 120 ns pulses separated by 1200 ns. The power in each case was adjusted for maximum echo amplitude. Long pulses were needed because of the limited microwave power available at the resonator frequency. The pulse interval was chosen to separate the wide echo from any possible overlapping signal due to resonator ring-down. Table 1 provides comparison data.

### *Isolation*

Isolation between the two modes of 60 to 70 dB was routinely achieved when the resonator contained nonlossy samples or the 1-mm-od, aqueous solution of the Nycomed radical (*23*), placed in 4-mm-od quartz sample tubes. With deionized water in a 4-mm-od quartz sample tube, the isolation decreased to 52 dB.

### *FID*

There is intense interest in the use of narrow-line EPR signals for *in vivo* EPR spectroscopy and imaging at low frequencies. As a step toward optimizing such experiments, we are creating resonators at low microwave frequencies. This L-band resonator is on the path from the more common EPR microwave frequencies to RF frequencies at which penetration into living organisms is enhanced. The Nycomed trityl radical (*23*) is typical of the species being studied (*27*). Consequently, as a test of the performance of the L-band CLR we measured the free induction decay (FID) of an aqueous solution of the Nycomed radical (Fig. 2). The sample was in a ca. 1-mm-od

**TABLE 1**
**CLR Dimensions and Test Result Summary**

| | L-band CLR | S-band CLR |
|---|---|---|
| Sample loop diameter | 4.2 mm | 4.2 mm |
| Sample loop length | 15 mm | 12.7 mm |
| Size of the sample region common to both loops | SL = 6 mm<br>SW = 3.2 mm | SL = 6 mm<br>SW = 2.54 mm |
| Frequency, critically coupled | 1.911 GHz | 3.100 GHz |
| $Q_L$, critically coupled (fixed-, variable-frequency) | 329, 313 | 570, 520 |
| Echo amplitude at $\tau$ = 1200 ns | 536 mV | 1240 mV |
| Relative system gain | −0.8 dB | 0 dB |
| Adjusted echo amplitude | 489 mV | 1240 mV |
| Echo amplitude ratio (S/L) | 1 | 2.5 |
| Echo amplitude ratio predicted based on 7/4 power of frequency (*25, 26*) and ratio of filling factors | 1 | 2.5 |

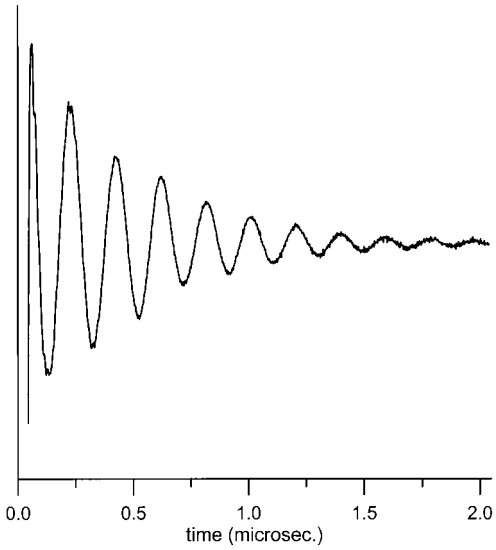


**FIG. 2.** Free induction decay (FID) of air-saturated aqueous solution of the Nycomed trityl radical in a ca. 1-mm-od sample tube. The FID was recorded in a LeCroy digital oscilloscope (Model 9310A, 400-MHz bandwidth), starting immediately after the spectrometer dead time.

glass capillary tube, placed inside a standard 4-mm-od quartz sample tube, without any special support to position the capillary vertically. This created a potential disturbance of microwaves that might be expected to reduce the isolation of the two modes. The significance of this measurement is the short dead time, discussed in the next paragraph, and the high isolation (60 dB) achieved with an aqueous sample nonsymmetically supported in the resonator.

*Dead Time*

The dead time was measured in two operating modes, with the CLR overcoupled to a $Q \approx 30$. In practice, in a two-pulse ESE experiment switching times in the microwave circuit limits the shortest time between pulses and, hence, the shortest time at which an echo can be acquired. This time was 45 ns when the first pulse was 50 ns long and decreased to 33 ns when the first pulse was 40 ns long, as in Fig. 3. Note that, in the ESE measurement, phase cycling is used to cancel the FID, and this also cancels some of the resonator ring-down. When only one microwave pulse was used, as in an FID experiment, some of the spectrometer limitations are removed, phase cycling was not used, and the resonator ring-down dominates the spectrometer dead time. Since the ring-down is exponential, the measure of the dead time is somewhat arbitrary. Based on observation of the FID on an oscilloscope, we judged that there was no significant interference of the ring-down with the FID after 60 ns following the end of the pulse. For a weaker signal the interference would be significant at longer times, and in this case a background subtraction would be necessary. Such subtraction is feasible so long as the combined EPR signal and ring-down do not exceed the dynamic range of the amplifiers or digitizer. Using a criterion of ability to subtract the background, one could cite a dead time shorter than 60 ns for this resonator.

*ESE Decay*

The depth of nuclear modulation in electron spin echo signals (ESEEM) is inversely proportional to the square of the magnetic field (hence, microwave frequency for $g \approx 2$) and is often so deep at low frequencies that it is difficult to record the ESEEM. For the same resonator $Q$, dead time is inversely proportional to microwave frequency, so dead time is five times longer at 1.8 GHz than at 9.2 GHz. Long dead time may cause failure to observe an important modulation in the ESEEM. In cosine Fourier transforms of the time domain EPR data, the dead time can cause oscillations in the frequency domain that may result in ambiguities in assigning characteristic frequencies. Consequently, reduction of the dead time is important for ESEEM. In principle, the CLR results in reduction of dead time by about seven time constants due to the $>$60-dB isolation of the signal voltage from the effect of pump power leakage.

## CONCLUSIONS

The CLR design, previously demonstrated at S-band, works at least as well at L-band. The isolation achieved between

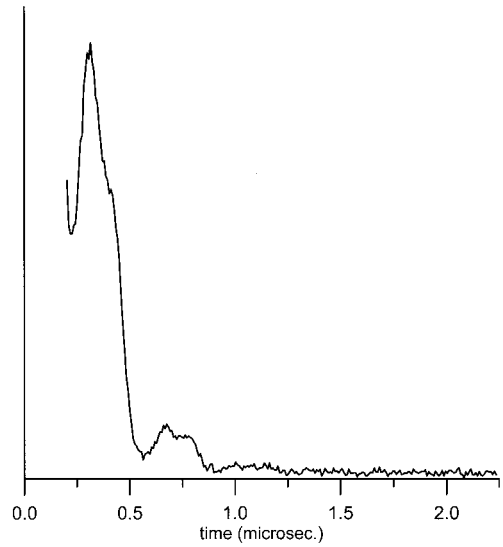


**FIG. 3.** Two-pulse electron spin echo (ESE) decay of a sample of coal (U.S. National Bureau of Standards Standard Reference Material 1635). Microwave pulse lengths were 40 and 80 ns, which were approximately 90 and 180° pulses at the full power available at this microwave frequency. Data collection began 53 ns after the end of the second pulse. The time axis includes effects of finite pulse widths. The off-resonance background signal, due to instrumental artifacts, was subtracted from the on-resonance signal. The boxcar aperture of ca. 100 ns was centered on the top of the echo. The proton modulation is deep, as expected at L-band. The short dead time permitted acquisition of the first minimum in the modulation pattern.

modes makes feasible pulsed ESE and FID spectroscopy with short relaxation times and deep modulation even at L-band. Within the accuracy of the measurements, the comparison of echo intensities using the same sample in S-band and L-band CLRs is consistent with our predictions (*25, 26*) of the frequency dependence of EPR signal intensities (Table 1).

## ACKNOWLEDGMENTS

The development of this resonator was supported by NIH Grant R01 RR12183 and the University of Washington. The specific design was stimulated by the research needs of Dr. Colin Mailer, University of Washington, who also prepared the solution of the Nycomed radical used in Fig. 2. The Nycomed radical was provided by Nycomed Innovation, Malmö, Sweden, to Dr. Howard Halpern, University of Chicago, whom we thank. We thank Professor Sandra S. Eaton for writing the data collection software and for assistance in preparation of the manuscript.

## REFERENCES

1. A. M. Portis and D. Teaney, Microwave Faraday rotation: Design and analysis of a bimodal cavity. *J. Appl. Physics.* **29,** 1692–1698 (1958).
2. D. T. Teaney, M. P. Klein, and A. M. Portis, Microwave superheterodyne induction spectrometer. *Rev. Sci. Instrum.* **32,** 721–729 (1961).
3. C. Franconi, Microwave cavity analogs of Bloch inductors. *Rev. Sci. Instrum.* **41,** 148–149 (1970).
4. J. S. Hyde, J. C. W. Chien, and J. H. Freed, Electron–electron double resonance of free radicals in solution. *J. Chem. Phys.* **48,** 4211–4226 (1968).
5. J. S. Hyde, L. D. Kispert, R. C. Sneed, and J. C. W. Chien, Frequency-swept electron–electron double resonance: Separation of overlapping spectra in irradiated malonic acid. *J. Chem. Phys.* **48,** 3824–3825 (1968).
6. J. S. Hyde, R. C. Sneed, Jr., and G. H. Rist, Frequency-swept electron-electron double resonance: DPPH in liquid and frozen solution. *J. Chem. Phys.* **51,** 1404–1416 (1969).
7. J. S. Hyde, ELDOR spectroscopy, *in* "Foundations of Modern EPR" (G. R. Eaton, S. S. Eaton, and K. M. Salikhov, Eds.), Chap. H.10, World Scientific, Singapore (1998).
8. R. C. Sneed, Jr., Bimodal cavity resonator for microwave spectrometers. U.S. Patent 3,609,520, September 28, 1971.
9. W. S. Moore, The Design, analysis, and performance of resonant and non-resonant microwave transmission devices with theoretically infinite rejection. *Rev. Sci. Instrum.* **44,** 158–164 (1973).
10. M. Huisjen and J. S. Hyde, A pulsed EPR spectrometer. *Rev. Sci. Instrum.* **45,** 669–675 (1974).
11. D. S. Leniart, Instrumentation and experimental methods in double resonance, *in* "Multiple Electron Resonance Spectroscopy" (M. M. Dorio and J. H. Freed, Eds.), Chap. 2, Plenum, New York (1979).
12. C. Mailer, H. Thomann, B. H. Robinson, and L. R. Dalton, Crossed $TM_{110}$ bimodal cavity for measurement of dispersion electron paramagnetic resonance and saturation transfer electron paramagnetic resonance signals for biological materials. *Rev. Sci. Instrum.* **51,** 1714–1721 (1980).
13. W. Barendswaard, J. A. M. Disselhorst, and J. Schmidt, A bimodal cavity for reducing the dead-time in electron spin-echo spectroscopy. *J. Magn. Reson.* **58,** 477–483 (1984).
14. R. Biehl and D. Schmalbein, Resonator for electron spin resonance experiments. U.S. Patent 4,314,204, February 2, 1982.
15. J. S. Hyde and W. Froncisz, Loop–gap resonators, *in* "Advanced EPR: Applications in Biology and Biochemistry" (A. J. Hoff, Ed.), Chap. 7, pp. 277 ff, Elsevier, Amsterdam (1989).
16. A. I. Tsapin, J. S. Hyde, and W. Froncisz, Bimodal loop–gap resonator. *J. Magn. Reson.* **100,** 484–490 (1992).
17. W. Piasecki, W. Froncisz, and J. S. Hyde, Bimodal loop–gap resonator. *Rev. Sci. Instrum.* **67,** 1896–1904 (1996). (Presented at the Workshop on Loop–Gap Resonators, Biomedical ESR Center, Milwaukee, WI, May 1995.)
18. G. A. Rinard, R. W. Quine, B. T. Ghim, S. S. Eaton, and G. R. Eaton, Easily tunable crossed-loop (bimodal) EPR resonator, *J. Magn. Reson. A* **122,** 50–57 (1996).
19. G. A. Rinard, R. W. Quine, B. T. Ghim, S. S. Eaton, and G. R. Eaton, Dispersion and superheterodyne EPR using a bimodal resonator, *J. Magn. Reson. A* **122,** 58–63 (1996).
20. L. R. Dalton, Ed., "EPR and Advanced EPR Studies of Biological Systems," pp. 142 ff, CRC Press, Boca Raton, FL (1985).
21. C. P. Poole, Jr., "Electron Spin Resonance," 2nd ed., Wiley, New York (1983).
22. B.-K. Na, S. I. Kelly, M. A. Vannice, and A. B. Walters, Development of the microwave Hall effect technique using an ESR spectrometer and a network analyser. *Meas. Sci. Technol.* **2,** 770–779 (1991), and references therein.
23. J. H. Ardenkjaer-Larsen, I. Laursen, I. Leunbach, G. Ehnholm, L-G. Wistrand, J. S. Petersson, and K. Golman, EPR and DNP properties of certain novel single electron contrast agents intended for oximetric imaging. *J. Magn. Reson.* **133,** 1–12 (1998).
24. S. S. Eaton and G. R. Eaton, Irradiated fused quartz standard sample for time domain EPR, *J. Magn. Reson. A* **102,** 354–356 (1993).
25. G. A. Rinard, R. W. Quine, R. Song, G. R. Eaton, and S. S. Eaton, Absolute EPR spin echo and noise intensities, *J. Magn. Reson.* **140,** 69–83 (1999).
26. G. R. Eaton, S. S. Eaton, and G. A. Rinard, Frequency dependence of EPR sensitivity, *in* "Spatially Resolved Magnetic Resonance: Methods, Materials, Medicine, Biology, Rheology, Geology, Ecology, Hardware" (P. Blümler, B. Blümich, R. Botto, and E. Fukushima, Eds.), p. 65–74, Wiley-VCH, Weinham (1998).
27. R. Murugesan, J. A. Cook, N. Devasahayam, M. Afeworki, S. Subramanian, R. Tschudin, J. A. Larsen, J. B. Mitchell, A. Russo, and M. C. Krishna, In vivo imaging of a stable paramagnetic probe by pulsed-radiofrequency electron paramagnetic resonance spectroscopy. *Magn. Reson. Med.* **38,** 409–414 (1997).